Simulation and Analysis of the Influence of the Support Structure on a Wind Turbine Gear Set

Eduardo Paiva Okabe[1(✉)] and Pierangelo Masarati[2]

[1] School of Applied Sciences, University of Campinas - UNICAMP, PO Box 1068, Limeira, Brazil
eduardo.okabe@fca.unicamp.br

[2] Dipartimento di Scienze e Tecnologie Aerospaziali, Politecnico di Milano, Via La Masa 34, 20156 Milano, Italy
pierangelo.masarati@polimi.it

Abstract. This work presents the numerical modeling, simulation and analysis of a wind turbine gearset supported by a flexible structure model. Gearboxes based on epicyclic gear trains applied to wind turbines have some advantages, i.e., compactness, robustness and low maintenance requirements. The gearbox is one of its main components because it is responsible for transforming the low angular speed of the rotor into the higher operation speed of the induction generator. Failures in this component cause loss of efficiency and directly impact the energy generated. The gearbox is attached to the nacelle, which is supported by the wind turbine tower. Wind gusts and shear can cause vibration that affects the tower and the nacelle and, therefore, all the components attached to them. To model these phenomena, a detailed model of a 600 kW turbine was built using the MBDyn software. The bearing, gear and the induction generator models were implemented as user-defined modules and were further integrated into the complete model of the wind turbine. Results showed that the gearbox components were affected by the dynamic behavior of the support structure and, therefore, its influence should be accounted for in the design of wind turbines.

Keywords: Wind turbine gearbox · Support structure
Multibody dynamics

1 Introduction

The use of wind power has the advantages of being a clean, sustainable, and cost effective source of energy. Moreover, wind turbines can be built on rural areas providing additional income to the landowners [21]. Wind technology is driving towards the direction of the cost reduction in wind power. As a result of it, rotor diameters are increasing and towers are getting taller and more flexible, which is demanding a reduction of relative size, mass and cost of the drivetrains.

K. L. Cavalca and H. I. Weber (Eds.): IFToMM 2018, MMS 63, pp. 518–530, 2019.
https://doi.org/10.1007/978-3-319-99272-3_36

Compared to the traditional fossil fired turbines [10], the initial investment cost of the wind turbine unit is higher. According to [21], the drivetrain cost is about 40% of the total installed costs. Although there are systems that eliminate the gearbox of the drivetrain, like the direct-drive ones, they are more expensive and heavier [13,18]. Therefore, the study and improvement of turbine gear sets and the further increase of their lifespans can bring opportunities for considerable economic savings.

Wind turbines are subjected to internal and external vibrations like any other rotating machinery [4,7], which compromise their performance and can increase the maintenance cost and downtime [15]. Cavalca et al. [3] investigated the influence of the support structure on rotor-bearing system showing that the effects of support structure are stronger in the connection points, which were the hydrodynamic bearings in this case.

Adhikari and Bhattacharya [1] investigated the effect of flexible foundations on wind turbine towers. They modeled the tower as an Euler-Bernoulli beam with elastic end support to simulate the flexibility of the foundation. As one would expect, the results showed that the natural frequency of the tower decreased by lowering the stiffness of the foundation or increasing the axial load.

Rachholz et al. [19] used a multibody model to analyze the effect of a lattice tower on the dynamic behavior of a 2 MW wind turbine. The lattice structure was modeled using a finite element software and the model reduced to a low-frequency equivalent modal basis using the Craig Bampton method. They concluded that the behavior of the turbine is largely dependent on the damping of the structure.

Another important component in wind turbines is the generator, which is responsible for converting mechanical into electrical energy. The generator is the interface between the turbine and the electrical network; therefore, it transmits mechanical problems to the electrical grid and vice-versa.

One of the most used types of generator in wind turbines is based on induction machines, specifically single and double squirrel cage generators [14]. This type of generators have fewer mechanical components, and do not need commutators, because they use the alternating current to generate the magnetic field in the stator, which extracts power from the rotor rotation.

To simulate the gearbox of a wind turbine with aerodynamic elements and an induction machine, a simulation platform is needed that can deal with different physical domains, hence their mathematical models have been implemented using the multibody/multiphysics simulation software MBDyn, which is open source and constantly maintained and updated by its developers. It would be very difficult to implement these models using a commercial multibody software, because one would need to depend on the type of user-defined routines that are explicitly supported by the software, which usually are very restricted and may have lower performance than those of the built-in libraries.

One of the main advantages of modeling components in a integrated way with MBDyn is the versatility of using them to model different machines, such as an electric bus transmission, a combustion engine or a metal lathe.

2 Methodology

A mechanical constrained system can be formulated as a system of Differential-Algebraic Equations (DAE) [12]:

$$\begin{aligned} \mathbf{M}\dot{\mathbf{q}} - \boldsymbol{\beta} &= \mathbf{0} \\ \dot{\boldsymbol{\beta}} + \left(\frac{\partial \boldsymbol{\phi}}{\partial \mathbf{q}}\right)^T \boldsymbol{\lambda}_\phi + \left(\frac{\partial \boldsymbol{\psi}}{\partial \dot{\mathbf{q}}}\right)^T \boldsymbol{\lambda}_\psi &= \sum \mathbf{f}\left(\mathbf{q}, \dot{\mathbf{q}}, t\right) \\ \boldsymbol{\phi}\left(\mathbf{q}, t\right) &= \mathbf{0} \\ \boldsymbol{\psi}\left(\mathbf{q}, \dot{\mathbf{q}}, t\right) &= \mathbf{0} \end{aligned} \tag{1}$$

where $\mathbf{M}$ is the inertia matrix, $\boldsymbol{\beta}$ is the momentum vector, $\mathbf{q}$ is the position vector, $\boldsymbol{\phi}$ is the system of holonomic constraint equations, $\boldsymbol{\psi}$ is the system of non-holonomic constraint equations, $\boldsymbol{\lambda}_\phi$ is the vector of Lagrange multipliers associated with the holonomic constraints, $\boldsymbol{\lambda}_\psi$ is the vector of Lagrange multipliers associated with the non-holonomic constraints, $\mathbf{f}$ is the vector of external loads, and $\dot{(\clubsuit)}$ represents the time derivative of $(\clubsuit)$.

Dynamic systems in MBDyn are based on nodes, like the ones used in finite element algorithms. Nodes provide degrees of freedom; they can be associated with different physical domains, such as mechanical, thermal and electrical. This structure makes it easier to integrate different components of the same machine in a monolithic simulation.

For example, the induction machine model presented in this work integrates dynamic structural and electric nodes in one element, that supports the simulation of the interaction between mechanical and electrical domains.

Constraints and forces have to be applied on nodes, thus they become part of the modeled system. This is performed by adding two sets of equations to the variables associated with each node. The first set is used in the assembly of the system of equations (1), and the second set is used during the nonlinear solution phase, if it is necessary.

The rolling bearings and the gear tooth mesh are considered as external loads in vector $\mathbf{f}$, whereas the generator (induction machine) adds a set of equations to the holonomic constraints which connect structural and electric nodes.

The gear meshing model is essential to understand the dynamic behavior of the gearbox, hence its modeling is going to be detailed in the next section.

2.1 Gear Modeling

The contact force between gear teeth can be modeled using a spring-damper equation:

$$F_g = K s_n + C \dot{s}_n \tag{2}$$

where F_g is the force generated by the contact of the teeth, K and C are respectively the stiffness and damping related to this contact, and s_n is the teeth surface penetration.

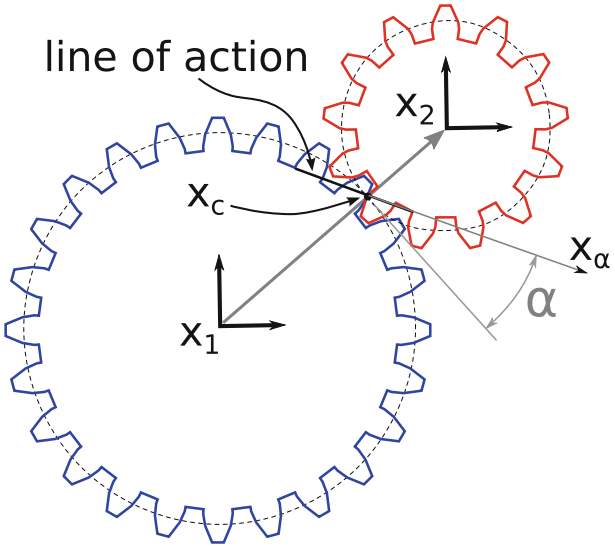

Fig. 1. Gear reference system.

To use this contact force in MBDyn's multibody environment, this force has to be applied to the nodes associated with the gears of the pair, which can be seen in Fig. 1. Therefore, these forces and moments generated by the contact can be expressed as:

$$\begin{aligned} \mathbf{F}_1 &= -F_g \mathbf{R}_c \mathbf{x}_\alpha \\ \mathbf{F}_2 &= \mathbf{F}_1 \\ \mathbf{C}_1 &= F_g \cos\alpha \cdot r_1 \mathbf{R}_c \mathbf{e} \\ \mathbf{C}_2 &= F_g \cos\alpha \cdot r_2 \mathbf{R}_c \mathbf{e} \end{aligned} \tag{3}$$

where $\mathbf{F}_i$ and $\mathbf{C}_i$ are the vectors of the force and the moment applied to the ith node, $\mathbf{R}_c$ is the orientation matrix related to the contact direction, $\mathbf{x}_\alpha$ is the vector that represents the force line of action, α is the pressure angle, r_i is the pitch radius of the gear associated with the ith node, and $\mathbf{e}$ is the vector associated with the rotation axis of the gears. The surface penetration s_n can be deduced using the formulation proposed by Lin and Parker [9] and adapting it to the multibody kinematics. Therefore, the displacement of each gear has to be projected along the line of action, which is calculated using the dot product of the displacement and line of action vectors. The calculation also includes the rotation of each gear; then, the surface penetration can be written as:

$$s_n = \mathbf{R}_c \mathbf{x}_\alpha \cdot (\mathbf{x}_1 - \mathbf{R}_c \tilde{\mathbf{x}}_1 - \mathbf{x}_c) - \mathbf{R}_c \mathbf{x}_\alpha \cdot (\mathbf{x}_2 - \mathbf{R}_c \tilde{\mathbf{x}}_2 - \mathbf{x}_c) + r_1 \boldsymbol{\theta}_{1c} \cdot \mathbf{e} + r_2 \boldsymbol{\theta}_{2c} \cdot \mathbf{e} \tag{4}$$

where $\mathbf{x}_i$ is the position of the ith node, $\mathbf{x}_c$ is the position of the point of contact, r_i is the primitive radius of the gear attached to the ith node, and θ_{ic} is the Euler

parameters vector, or orientation vector, associated with the relative rotation of the ith node concerning the contact direction. The position offset $\tilde{\mathbf{x}}_i$ is used when the center of the rotation axis is not coincident with the center of the node. The Euler parameters vector can be calculated according to

$$\boldsymbol{\theta}_{ic} = \mathrm{ax}(\exp^{-1}(\mathbf{R}_c^T \mathbf{R}_i)) \tag{5}$$

where operator ax(♣) extracts the axial of matrix (♣) (i.e. the vector that expresses its skew-symmetric part), $\mathbf{R}_i$ is the rotation matrix related to the ith node, and exp(♣) is the exponential map operator that expresses the orientation matrix (♣) from the corresponding orientation vector.

To calculate the damping contribution, Eq. 4 needs to be differentiated with respect to time:

$$\begin{aligned}
\dot{s}_n = {} & \boldsymbol{\omega}_c \times \mathbf{R}_c \mathbf{x}_\alpha \cdot (\mathbf{x}_1 - \mathbf{R}_c \tilde{\mathbf{x}}_1 - \mathbf{x}_c) + \mathbf{R}_c \mathbf{x}_\alpha \cdot (\dot{\mathbf{x}}_1 - \boldsymbol{\omega}_c \times \mathbf{R}_c \tilde{\mathbf{x}}_1 - \dot{\mathbf{x}}_c) - \\
& \boldsymbol{\omega}_c \times \mathbf{R}_c \mathbf{x}_\alpha \cdot (\mathbf{x}_2 - \mathbf{R}_c \tilde{\mathbf{x}}_2 - \mathbf{x}_c) - \mathbf{R}_c \mathbf{x}_\alpha \cdot (\dot{\mathbf{x}}_2 - \boldsymbol{\omega}_c \times \mathbf{R}_c \tilde{\mathbf{x}}_2 - \dot{\mathbf{x}}_c) + \\
& r_1 \boldsymbol{\omega}_{1c} \cdot \mathbf{e} + r_2 \boldsymbol{\omega}_{2c} \cdot \mathbf{e} \\
\boldsymbol{\omega}_{1c} = {} & \mathbf{R}_c^T (\boldsymbol{\omega}_1 - \boldsymbol{\omega}_c) \\
\boldsymbol{\omega}_{2c} = {} & \mathbf{R}_c^T (\boldsymbol{\omega}_2 - \boldsymbol{\omega}_c)
\end{aligned} \tag{6}$$

where $\boldsymbol{\omega}_c$ is the angular velocity vector related to the reference that defines the contact direction, $\boldsymbol{\omega}_1$ and $\boldsymbol{\omega}_2$ are the angular velocity vectors of nodes 1 and 2, the dot ($\dot{\clubsuit}$) represents the time derivative of (♣). This formulation was implemented in C++ and included as a user-defined, run-time loadable module of MBDyn. Modules have the same performance of built-in elements.

3 Wind Turbine Modeling

The model is based on NREL's CART 600 kW turbine developed by Stol [20]. The actual turbine is showed in Fig. 2. This model was further adapted to MBDyn by Cavagna et al. [2] to simulate the turbine in a real-time environment (RTAI/MBDyn).

The flexible structure (tower) that supports the nacelle was modeled as a beam using the finite-volume element developed by Ghiringhelli et al. [5]. In the present model, the tower uses five three-node beam elements, for a total of 11 structural nodes. Its lower end is clamped to the ground and the upper one is rigidly connected to the nacelle.

The other components of this turbine model are:

- the nacelle, modeled as a rigid body connected to the tower by a yaw hinge. The yaw motion is constrained by an extremely stiff deformation joint, since no control or actuation on the yaw degree of freedom is considered in the analysis;
- the low-speed shaft, also modeled as a rigid body supported by rigid bearings; a total joint [11] connects the shaft to the input of the gearbox, transmitting only the torque;

Fig. 2. Controls Advanced Research Turbine (CART) [20].

- the two blades, modeled as aerodynamic beams coupled with finite-volume beam elements; each of them is fixed to the teetering hub through a revolute hinge that accounts for pitch rotation;
- the generator, based on a induction machine model developed by Krause et al. [8], that was recently adapted to the multibody systems by Okabe et al. [16]. It consists of a three-phase induction machine that uses the direct-quadrature (dq) transformation to eliminate all time-varying inductances from the tension equations. The electromagnetic moment is applied to rotor and stator, and the electrical voltage and current are supplied by the induction machine to electric nodes. The generator is connected to the output shaft of the gearbox by a viscous deformable joint that mimics a hydraulic power transmission.

The gearbox, which is the focus of this work, is shown in Fig. 3. It is a resized version of the gearbox model studied by Okabe and Masarati [17]. The main properties of gearbox and generator are presented in Table 1.

The components of the gearbox were modeled as rigid bodies in a three dimensional space subjected to gravity. Gears are meshed to each other through the viscoelastic model presented in the previous section. The pressure angle was kept constant (20°) and the relative position and rotation were used to calculate

Table 1. Properties of gearbox and induction generator.

Part	Parameter	Value
Planet carrier	Mass	1300 kg
	Moment of inertia - Ixx	188 kg/m^2
	Moment of inertia - Iyy/Izz	128 kg/m^2
Planetary shaft	Internal diameter	100 mm
	External diameter	175 mm
	Length	450 mm
Sun shaft	Internal diameter	75 mm
	External diameter	125 mm
	Length	470 mm
Output shaft	Diameter	80 mm
	Length	300 mm
Ring gear	Teeth number	93
Planet gear "A"	Teeth number	22
	Internal diameter	175 mm
Ring/Planet "A"	Module	10 mm
	Facewidth	150 mm
Planet gear "B"	Teeth number	103
	Internal diameter	175 mm
Sun gear	Teeth number	29
Planet "B"/Sun	Module	5.38 mm
	Facewidth	150 mm
Gear 1 (output)	Teeth number	57
	Internal diameter	80 mm
Gear 2 (output)	Teeth number	23
	Internal diameter	80 mm
Gear 1/Gear 2	Module	5.5 mm
	Facewidth	56 mm
Gear mesh	Stiffness	10^8 N/m
	Damping	10^4 Ns/m
Generator	Number of phases	3
	Frequency	60 Hz
	Voltage	575 V
	Number of poles	4
	Stator resistance R_s	0.00053 Ω
	Rotor resistance R'_r	0.00048 Ω
	Stator inductance L_{ls}	0.0365 mH
	Rotor inductance L'_{lr}	0.052 mH
	Magnetizing inductance L_M	1.97 mH

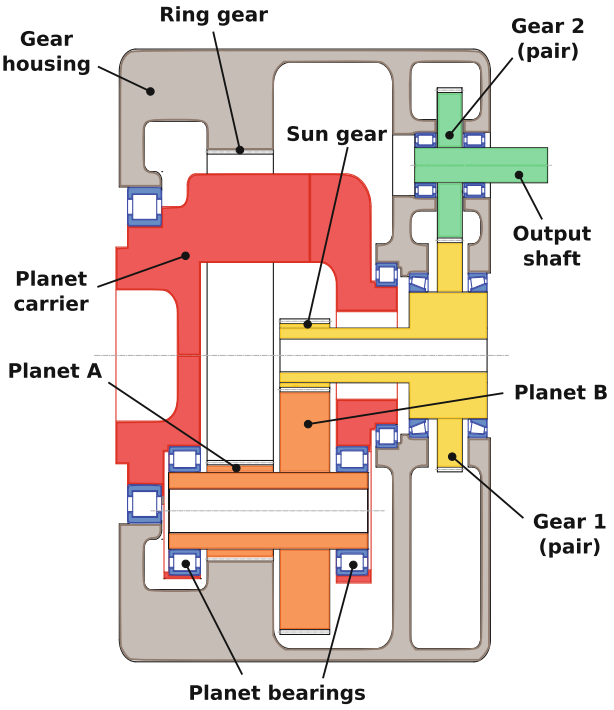

Fig. 3. Cross sectional drawing of the gearbox (adapted from [17]).

the contact force. The gear model does not consider the backlash, which means that there are no gaps between the teeth.

The gearbox shafts are supported by roller bearings modeled by the semi-empirical equation proposed by Gargiulo and reported by Hambric et al. [6].

4 Results

Figure 4 (left) shows the orbit of the carrier shaft inside the bearing close to the input. The circular motion is related to the orbital displacement of the planet gears. The increase of the transmitted power from 270 to 600 kW forces the carrier down, which is associated with the vertical component of the mesh force in the final gear pair.

The effect of the flexible tower structure is quite evident, because it introduces a strong oscillation in the orbit. The frequency of this vibration is 7.3 Hz, which can be seen in Fig. 4 (right). There are some harmonics related to this vibration at 14.4 and 21.8 Hz, but they have much less power and, therefore, they cannot be seen in the orbit plot.

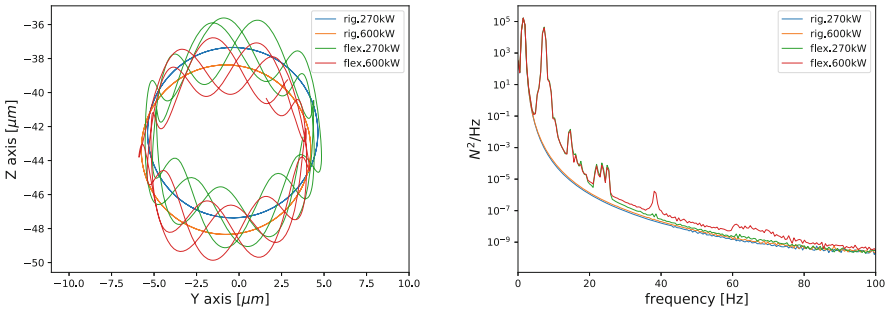

Fig. 4. Orbit of the carrier shaft on the bearing (left) and power spectral density of the vertical force in this bearing (right).

Figure 5 (left) shows the orbit of the planet shaft inside the roller bearing. The orbit of all planets are very similar; therefore, only the orbit of the planet that starts the movement on the top of the carrier is shown here. The locus of the orbit is affected by the power transmitted; the amplitude is much smaller when compared to the carrier shaft displacement. They are also influenced by the flexibility of the structure (Fig. 5, right) but instead of one peak there are two at 6.3 and 7.8 Hz, and there is one that can be considered a harmonic at 20.1 Hz.

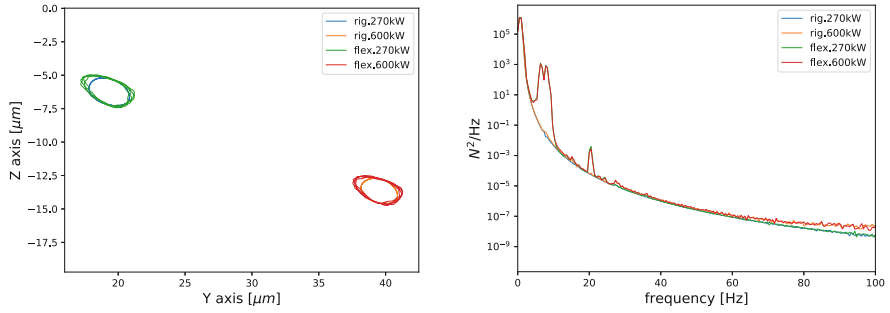

Fig. 5. Orbit of the planet shaft on the bearing (left) and power spectral density of the vertical force in this bearing (right).

Observing the orbit of the sun gear shaft presented in Fig. 6 (left), one can notice that the orbits decreased but they still have the locus displacement related to the power transmission. The power spectral density of the vertical force in Fig. 6 (right) shows that the structure has a stronger influence on the sun gear shaft than the planet shat, because its bearings are fixed to the gear housing, which in turn is rigidly attached to the nacelle.

Figure 7 shows the orbit of the output shaft. It is quite small (around 1 μm) and slanted due to the pressure angle of the gears. Analyzing the vertical force

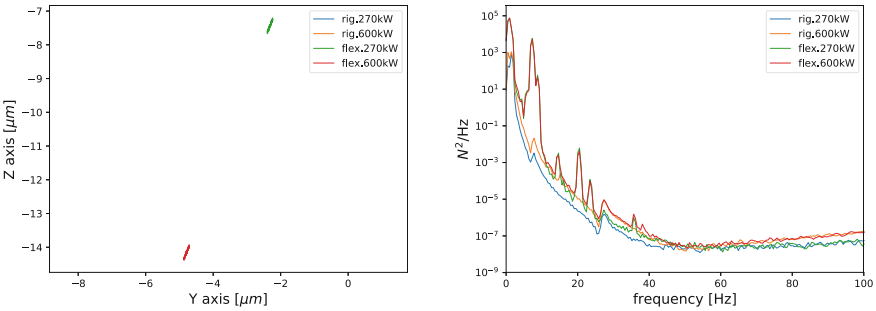

Fig. 6. Orbit of the sun shaft on the bearing (left) and power spectral density of the vertical force in this bearing (right).

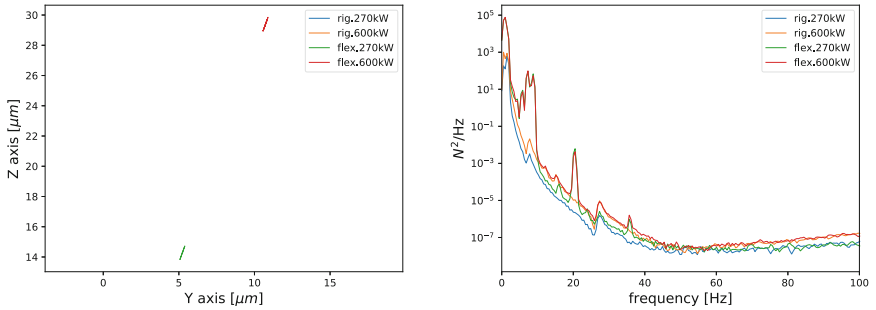

Fig. 7. Orbit of the output shaft on the bearing (left) and power spectral density of the vertical force in this bearing (right).

presented in Fig. 7 (right), one can notice that the vibration of the structure has an influence on the output bearing, because of its connection to the gear housing.

Another important aspect of the gearbox behavior is the torsional vibration, which can be analyzed through the rotational speed of its components. Figure 8 shows that the flexibility of the structure has a small influence on the rotational vibration of the carrier. There are two peaks at 6.3 Hz and 7.8 Hz that are associated with the structure, which was previously seen in the PSD plot of the planet shaft (Fig. 5).

The power spectral density of the planet gear rotational velocity (Fig. 8) shows peaks at slightly higher frequencies: 7.3 Hz and 9.7 Hz.

Figure 9 (left/right) show the power spectral density of the angular velocity of the sun gear and output shaft. The highest frequency is related to the rotation speed (1x) of each component; that is the reason why it increases the frequency from the carrier to the output shaft. The frequency harmonics in the sun shaft are 7.3 Hz and 19.5 Hz. The frequency harmonics of the output shaft at 7.3 Hz, 22.8 Hz, and 37.5 Hz.

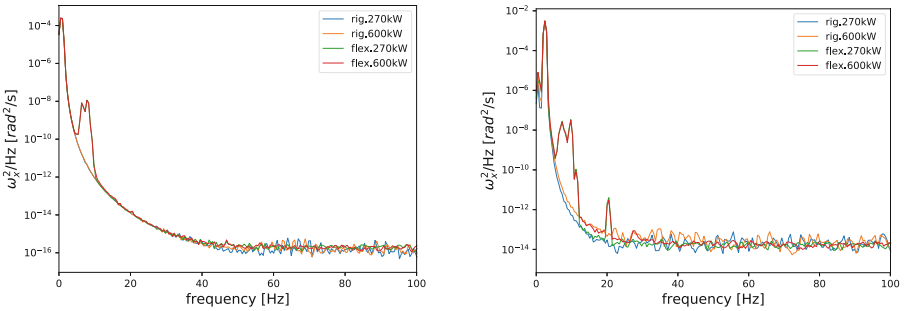

Fig. 8. Power spectral density of the angular velocity of the carrier (left) and planet shaft (right).

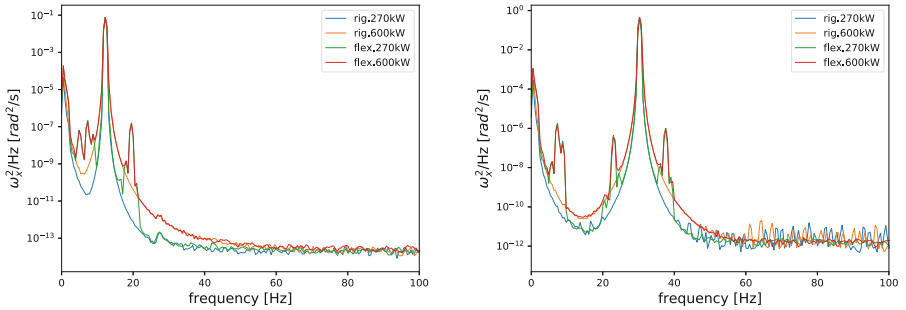

Fig. 9. Power spectral density of the angular velocity of the sun gear (left) and output shaft (right).

5 Conclusions

A complete model of a Wind Turbine was developed using a free software simulation platform to show the effects of a flexible support structure, namely the tower that carries the nacelle, on the gearbox dynamics. Simulations were performed at two different generated power levels; results were compared to those obtained using a rigid structure model.

The results showed that the vibration modes of the tower influence the displacement and force on the geartrain bearings. This represents an increase of approximately 10% of the load on the bearings.

A further development of the model will include the flexibility of the soil, that is known to influence the dynamic behavior of the tower structure and, hence it also influences the behavior of the gearbox. The interface of the tower and base is an important aspect of the structure dynamic behavior particularly due to the damping introduced in the system and, therefore, it should be included in the model.

References

1. Adhikari S, Bhattacharya S (2012) Dynamic analysis of wind turbine towers on flexible foundations. Shock Vibr 19(1):37–56
2. Cavagna L, Fumagalli A, Masarati P, Morandini M, Mantegazza P (2011) Real-time aeroservoelastic analysis of wind-turbines by free multibody software. In: Multibody dynamics. Springer, pp 69–86
3. Cavalca K, Cavalcante P, Okabe E (2005) An investigation on the influence of the supporting structure on the dynamics of the rotor system. Mech Syst Sig Process 19(1):157–174
4. Childs D (1993) Turbomachinery rotordynamics: phenomena, modeling, and analysis. Wiley, New York
5. Ghiringhelli GL, Masarati P, Mantegazza P (2000) A multibody implementation of finite volume C^0 beams. AIAA J 38(1):131–138
6. Hambric SA, Shepherd MR, Campbell RL, Hanford AD (2013) Simulations and measurements of the vibroacoustic effects of replacing rolling element bearings with journal bearings in a simple gearbox. J Vibr Acoust-Trans ASME 135(3):031012-1–031012-18
7. Kramer E (1993) Dynamics of rotors and foundations. Springer, New York
8. Krause PC, Wasynczuk O, Sudhoff SD, Pekarek S (2013) Analysis of electric machinery and drive systems, vol 75. Wiley, New York
9. Lin J, Parker RG (1999) Analytical characterization of the unique properties of planetary gear free vibration. J Vibr Acoust 121(3):316–321
10. Martin L (2010) Wind energy-the facts: a guide to the technology, economics and future of wind power. Routledge, London
11. Masarati P (2013) A formulation of kinematic constraints imposed by kinematic pairs using relative pose in vector form. Multibody Syst Dyn 29(2):119–137. https://doi.org/10.1007/s11044-012-9320-0
12. Masarati P, Morandini M, Mantegazza P (2014) An efficient formulation for general-purpose multibody/multiphysics analysis. J Comput Nonlinear Dyn 9(4) (2014). https://doi.org/10.1115/1.4025628
13. Morris L (2011) Direct drive vs. gearbox: progress on both fronts: will the wind turbine technology showdown leave just one technology standing? Power Eng 115(3):38–42
14. Müller S, Deicke M, De Doncker RW (2002) Doubly fed induction generator systems for wind turbines. IEEE Ind Appl Mag 8(3):26–33
15. Norton RL (1996) Machine design: an integrated approach. Prentice-Hall, New York
16. Okabe EP, Izuka J, Masarati P (2016) Modeling and simulation of a wind turbine gear set with hydrodynamic bearings attached to an induction generator. In: ASME 2016 international design engineering technical conferences and computers and information in engineering conference. American Society of Mechanical Engineers, p V006T09A029
17. Okabe EP, Masarati P (2014) Detailed modeling of wind turbine gear set by general-purpose multibody dynamics. In: Proceedings of the ASME 2014 international design engineering technical conferences, 17–20 August, DETC2014/MECH-34898
18. Polinder H, Van der Pijl FF, De Vilder GJ, Tavner PJ (2006) Comparison of direct-drive and geared generator concepts for wind turbines. IEEE Trans Energy Convers 21(3):725–733

19. Rachholz R, Woernle C, Staschko R (2015) Simulation of a small wind turbine with a bolted lattice tower under consideration of mass distribution and damping. In: Proceedings of the ECCOMAS thematic conference on multibody dynamics
20. Stol K (2003) Geometry and structural properties for the controls advanced research turbine (CART) from model tuning. NREL Report 32087
21. Zayas J, Derby M, Gilman P, Ananthan S (2015) Enabling wind power nationwide. Technical report, US Department of Energy